

# Simulating surface diffusion and surface growth in ceramics †

Mikhail Yu. Lavrentiev,<sup>a</sup> Duncan J. Harris,<sup>b</sup> John H. Harding,<sup>\*b</sup> Neil L. Allan<sup>a</sup> and John A. Purton<sup>c</sup>

<sup>a</sup> Department of Chemistry, University of Bristol, Cantocks Close, Bristol, UK BS8 1TS

<sup>b</sup> Department of Physics and Astronomy, University College London, Gower St., London, UK WC1E 6BT

<sup>c</sup> CCLRC Daresbury Laboratory, Daresbury, Cheshire, UK WA4 4AD

Received 23rd February 2004, Accepted 6th April 2004

First published as an Advance Article on the web 23rd July 2004

We examine the movement of ion pairs on the surfaces of simple oxides. Using temperature-accelerated dynamics the elementary processes involved are identified and the activation energies of these used as input to kinetic Monte Carlo simulations. Results are presented for the motion of BaO and SrO ion pairs on the (100) surfaces of BaO and SrO, respectively, and the formation of island pairs on these surfaces is studied. The simulations reveal the importance of *exchange* mechanisms in surface diffusion and growth of oxides. The importance of such reactions has been recognised previously for metallic surfaces but not for ionic systems, where it has been *assumed* that ionic surface diffusion is surface diffusion *via* the hopping motion of ion pairs from one surface site to another. Exchange mechanisms can dominate transport processes both on terraces and steps for both homoepitaxial and heteroepitaxial growth. We suggest the unavoidable mixing when an exchange mechanism operates must be considered when attempting to grow sharp interfaces in oxide nanostructures.

## Introduction

Well-defined layers of crystalline oxides on semiconductors are candidate materials for gate dielectrics in solid state electronics.<sup>1</sup> Such oxide layers are often grown using molecular beam epitaxy, and are usually required to be atomically smooth. The commonest smoothing mechanism is surface diffusion. This surface motion must not involve exchange with the surface, a process which necessarily involves surface mixing. Atomically sharp interfaces will be impossible to produce if the atoms of the surface layer swap places with those in the substrate below.

A recent review<sup>2</sup> on surface diffusion has drawn attention to the importance of exchange reactions at metallic surfaces.<sup>3</sup> Subsurface diffusion mechanisms have been proposed to explain the effects of surfactants<sup>3,4</sup> such as Pb on Cu. In marked contrast, all published work on ionic systems to our knowledge has assumed that ionic surface diffusion is *surface* diffusion, *i.e.* that an adsorbed ion pair is formed due to the Coulombic attraction between the ions and this pair moves from one surface site to another by a hopping mechanism, although intermixing of ions across an interface has been noted in high temperature molecular dynamics simulations.<sup>5</sup> Surface diffusion in ionic compounds has usually been assumed to take place *via* a simple mechanism in which an adsorbed ion pair forms on the surface and moves across it by a hopping mechanism. The possible rôles of other cooperative transport mechanisms have surprisingly been ignored.

Whilst it is possible to simulate the behaviour of superionic conductors directly using molecular dynamics,<sup>6</sup> in simple refractory oxides, in contrast, the barriers to migration are so high that the timescales required for direct simulation are prohibitive. When energy barriers are of the order of 1.5 eV or more, as is often the case in the bulk oxides, it is impossible to run molecular dynamics simulations for long enough to obtain adequate statistics at temperatures of interest. It is possible for kinetic Monte Carlo (KMC) methods to reach the relevant timescales, but these assume we know *in advance* the rates of *all* relevant mechanisms (see ref. 7 for developments here). One way of investigating a particular mechanism is to find the

activation pathway of a diffusion mechanism by a nudged elastic band method.<sup>8</sup> This requires knowledge of both the initial and final states of the diffusion mechanism. Also, some idea (however approximate) of the path of the trajectory itself is necessary so that a sensible set of initial configurations can be linked by the “elastic band” to ensure that the “nudging” of the band converges on the trajectory of the required mechanism. This presents no great problem for simple mononuclear systems like metals, but ionic materials are necessarily compounds and the increased complexity, reflected both in the list of possible mechanisms, the existence of long-range Coulombic forces and in the trajectory of any given mechanism, makes this approach impractical unless some information on the pathway can be provided.

A variety of methods have been proposed by Voter and coworkers<sup>9,10</sup> for situations where long timescales are required. These are usually referred to under the general label “accelerated dynamics” and provide a means of carrying out an *unbiased* calculation of the diffusion rate without any prior knowledge of the diffusion mechanism, *i.e.*, without advance information of the configuration of the final state or of the trajectory. Temperature accelerated dynamics (TAD) uses simulations performed at high temperature to calculate the evolution of systems at a lower temperature of interest. In contrast to extrapolations of high-temperature simulations to low temperature, it identifies and extrapolates the rates of individual mechanisms to lower temperatures, using the nudged elastic band method<sup>8</sup> to find the activation energy. Thereby, account is correctly taken of the different behaviour of the various contributing mechanisms with temperature. It is possible to use the TAD calculation as a direct simulation of the diffusion, by changing the state of the system according to the fastest mechanism and advancing the simulation clock by the shortest transition time at the required temperature. We use an alternative approach here. The method is used to collect an unbiased list of mechanisms and these together with the appropriate rates are input to a KMC simulation.

Barium oxide is of particular interest since this material has a dielectric constant high enough to be of use as a gate dielectric. In this paper we present results for the diffusion of BaO and SrO on the {100} surfaces of BaO and SrO, respectively, and show how these results can be used to study island growth on these surfaces.

† Based on the presentation given at Dalton Discussion No. 7, 5–7th July 2004, University of St Andrews, UK.

## Theoretical methods

### TAD

The aim of the TAD calculations is to increase the number of transitions undergone by the system by carrying out the simulations at a high temperature,  $T_{\text{high}}$ , while removing the transitions that should not have taken place at the lower temperature of interest,  $T_{\text{low}}$ . No prior information about the mechanisms is required. Each trajectory is free to explore the local potential surface and find its own escape route.

We start with the system in the basin on the potential energy surface corresponding to a particular local potential minimum. The system evolves at  $T_{\text{high}}$ . When it undergoes a transition out of the basin, as shown schematically in Fig. 1, the saddle point (the highest point on the minimum energy path) is found using the nudged elastic band method<sup>8</sup> and the corresponding static barrier height recorded. The trajectory is then reflected back into the basin, *i.e.*, the simulation is continued from the point where the trajectory crosses the dividing surface (DS) between the states A and B in Fig. 1 but with the velocities of all the particles reversed. Since a Langevin thermostat injects noise into the trajectory, the previous path is not retraced.

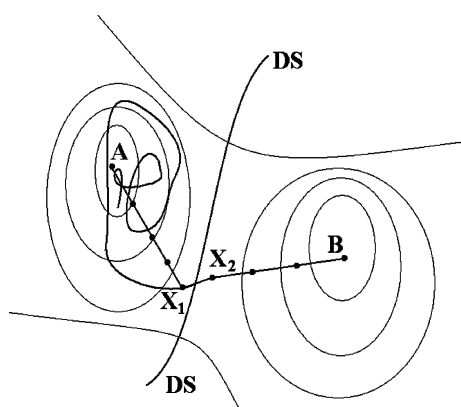


**Fig. 1** Implementation of the TAD method. The potential energy surface indicated by thin lines is crossed by the dividing surface separating states A and B (denoted by DS). The thick line shows the molecular dynamics trajectory starting in state A and crossing the dividing surface between  $X_1$  and  $X_2$ . When a transition into state B is detected, a discretized path A– $X_1$ – $X_2$ –B is constructed and optimised to a minimum energy path using the nudged elastic band method, giving the activation energy for the transition.

The TAD method assumes harmonic transition-state theory and thus the dependence of rates on temperature is exponential. Using the static barrier heights, we thus extrapolate each escape time at  $T_{\text{high}}$  to find the corresponding time at  $T_{\text{low}}$ , as shown schematically in Fig. 2. Knowledge of the pre-exponential factor is not required. Since the extrapolation to  $T_{\text{low}}$  can, as in Fig. 2, result in a reordering of escape times, a new shorter-time escape event (at  $T_{\text{low}}$ ) may be identified as the simulation continues at  $T_{\text{high}}$ . An additional assumption is the existence of a minimum prefactor,  $\nu_{\text{min}}$ . From this it is possible<sup>11</sup> to define a time  $t_{\text{high,stop}}$  at which the simulation from this basin can be stopped such that the probability that any transition observed after that time would replace the first transition at  $T_{\text{low}}$  is less than  $\delta$ .  $t_{\text{high,stop}}$  is given by

$$t_{\text{high,stop}} = \frac{\ln(1/\delta)}{\nu_{\text{min}}} \left( \frac{\nu_{\text{min}} t_{\text{low,short}}}{\ln(1/\delta)} \right)^{T_{\text{low}}/T_{\text{high}}} \quad (1)$$

where  $t_{\text{low,short}}$  is the shortest transition time at  $T_{\text{low}}$ . The minimum prefactor here was set to  $5 \times 10^{11}$  Hz. In a “normal” TAD calculation where the aim is to follow the diffusion directly, a higher value might be assigned to this quantity, but the objective here was to provide data for the KMC calculation

**Table 1** Short-range interionic potentials  $V(r) = A \exp(-r/\rho) - C/r^6$  for rock-salt oxides. The short-range term is ignored for cation–cation interactions. A cut-off of 9 Å was used in all cases

Interionic interactions	$A/\text{eV}$	$\rho/\text{Å}$	$C/\text{eV Å}^6$
$\text{Ba}^{2+}-\text{O}^{2-}$	905.7	0.3976	0.0
$\text{Sr}^{2+}-\text{O}^{2-}$	959.1	0.3721	0.0
$\text{O}^{2-}-\text{O}^{2-}$	22743.0	0.149	27.88

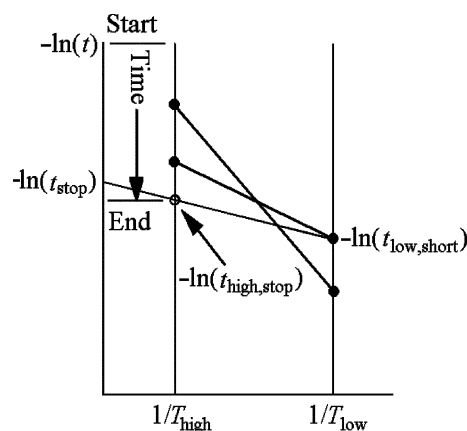


**Fig. 2** The TAD method, and the termination criterion (eqn. (1)). The molecular dynamics simulation time increases down the  $y$  axis as the simulation proceeds at temperature  $T_{\text{high}}$ . As the simulation progresses, new transitions (denoted by black circles on the high temperature axis) are found. Each time a transition is detected, the saddle point and the corresponding activation energy is found. The trajectory is reflected back into the region associated with minimum A (Fig. 1) and restarted from point  $X_1$ . The times of the transitions are transformed into low temperature transition times (circles on the low temperature axis). The line through the shortest low temperature transition time  $-\ln(t_{\text{low,short}})$  and  $-\ln(t_{\text{stop}}) = \ln(\nu_{\text{min}}/\ln(1/\delta))$  on the time axis, gives the time after which the simulation can be terminated on the high temperature axis,  $-\ln(t_{\text{high,stop}})$  such that  $\delta$  is the probability that any new transition observed after that time would be the fastest transition at  $T_{\text{low}}$ .

rather than follow the diffusion directly. Typically boosts of the order of  $10^2$ – $10^6$  were obtained for a given transition.

The TAD calculations are carried out using rigid ion potentials based on the well-established model of ref. 12. Full integral ionic charges are assumed, using the Ewald method<sup>13</sup> for the summation of the Coulombic interactions. Details of the short-range (non-Coulombic) interactions are given in Table 1. Models of this kind give excellent results for the surface energies and structures of oxides of simple closed-shell ions, defect energies and activation energies for ion transport.<sup>14</sup> Comparisons with quantum calculations show there is good agreement where appreciable redistribution of the electron density does not take place.<sup>15</sup>

Calculations were performed within the canonical ( $NVT$ ) ensemble. The surface was represented by a slab of ions ( $\approx 400$  ions), periodically repeated in three dimensions (with surface lattice vectors of 26.5 and 25.7 Å for BaO and SrO respectively), but with sufficient space between slabs in the third dimension to prevent inter-slab interactions. The slabs typically contained four layers, which is sufficient to ensure negligible interaction between the top and bottom layers of an individual slab. All ions in the slab are free to move.  $T_{\text{high}}$  and  $T_{\text{low}}$  were set to 1200 and 300 K, respectively.

### KMC

The set of possible movements of molecules on the surface and between the surface and the bulk, together with the corresponding activation energies from TAD calculations, allows us to run the KMC simulations. For each configuration of molecules on the surface, a set of possible events is established. The following were taken into account:

**Table 2** Activation energies for the processes used in the KMC simulations. The meaning of the symbols is explained in Fig. 3

Jump	Energy/eV
BaO(100) surface: Ba(ads) at F, O(ads) at G	
Ba(F:ads) $\rightarrow$ f	0.462
Ba(G:sfc) $\rightarrow$ c	
O(G:ads) $\rightarrow$ b	0.435
O(F:sfc) $\rightarrow$ e	
Ba(F:ads) $\rightarrow$ a	0.594
O(G:ads) $\rightarrow$ b	
BaO(100) surface: Ba(ads) at F, O at b and e	
O(e) $\rightarrow$ J:ads	0.369
O(b) $\rightarrow$ F:sfc	
BaO(100) surface: Ba at c and f, O(ads) at G	
Ba(f) $\rightarrow$ K:ads	0.352
Ba(c) $\rightarrow$ G:sfc	
BaO(100) surface: Ba at a, O at b	
Ba(a) $\rightarrow$ F:ads	0.468
O(b) $\rightarrow$ G:ads	
SrO(100) surface: Sr(ads) at F, O(ads) at G	
Sr(F:ads) $\rightarrow$ f	0.413
Sr(G:sfc) $\rightarrow$ c	
O(G:ads) $\rightarrow$ b	0.387
O(F:sfc) $\rightarrow$ e	
Sr(F:ads) $\rightarrow$ a	0.400
O(G:ads) $\rightarrow$ b	
SrO(100) surface: Sr(ads) at F, O at b and e	
O(e) $\rightarrow$ J:ads	0.378
O(b) $\rightarrow$ F:sfc	
SrO(100) surface: Sr at c and f, O(ads) at G	
Sr(f) $\rightarrow$ K:ads	0.358
Sr(c) $\rightarrow$ G:sfc	
SrO(100) surface: Sr at a, O at b	
Sr(a) $\rightarrow$ F:ads	0.335
O(b) $\rightarrow$ G:ads	

(i) Initial stage of the exchange jump – displacement of an ion (anion or cation) from the adsorbed layer towards the surface with simultaneous displacement of another ion of the same type from the surface towards the adsorbed layer. After this step both displaced ions occupy interstitial sites between the surface and the adsorbed layer.

(ii) Final stage of the exchange jump – movement of one of the displaced ions into the surface, and the other into the adsorbed layer;

(iii) Movement of an ion pair on the surface as a single species.

Activation energies for these events differ for movement near a step and away from it, in accordance with the TAD results. The rate of event is related to its activation energy according to  $\Gamma = \Gamma_0 \exp(-E_a/kT)$  where  $\Gamma_0$  is a characteristic vibrational frequency (taken to be  $10^{13} \text{ s}^{-1}$ ),  $E_a$  the activation energy and  $T$  the temperature. At each step, one of the possible events is randomly chosen with a probability proportional to its rate. The system is changed accordingly, and the time counter incremented<sup>7</sup> by  $\Delta t = -\ln \mu / \sum_i \Gamma_i$ , where  $\mu$  is a random number between 0 and 1, and  $\sum_i \Gamma_i$  is the sum over all possible events. The size of the surface in the KMC simulations was  $20 \times 20$  (*i.e.* 400 ions), with periodic boundary conditions applied. A typical simulation included  $4 \times 10^6$  events. Important activation energies for a single ion pair (BaO on BaO and SrO on SrO) related to the exchange mechanism of diffusion or to the movement of ion pair as a whole are collected together in Table 2. This table should be considered together with Fig. 3 which

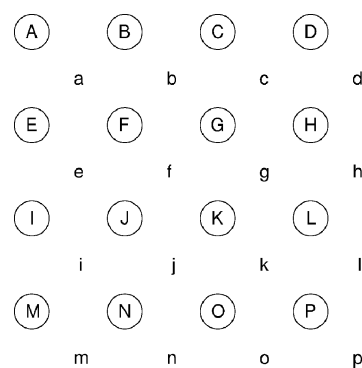


**Fig. 3** Labelling system for surface sites used in Table 2. Upper case letters refer to ion sites, lower case letters to interstitial sites. Key: ads = adsorbed atom above the surface; sfc = atom in surface layer. Example: Ba(F:ads)  $\rightarrow$  f – adsorbed Ba atom at position F moves to position f.

lists the various sites involved. In the presence of steps on the surface the number of possible events involving ion pairs increases dramatically.

## Results

We consider first the diffusion of BaO (SrO) ion pairs along the (100) surface of a BaO (SrO) substrate. The TAD calculations show clearly that the diffusion mechanism with the lowest energy barrier involves both cation and anion exchange with surface ions. Each jump involves one of the ions in the adsorbed ion pair exchanging with an ion of the same charge in the surface while the other atom of the adsorbed pair remains above, held in place by the Coulombic binding. The ion pair is thus reoriented by 90 or by 180°, depending on which of the three possible nearest-neighbour adsorption sites are occupied by the exchanged ion. The ion pair can then move by exchanging the counter-ion with a counter-ion in the surface in an analogous step. Diagrams of the exchange mechanism for oxygen diffusion are shown in Fig. 4(a)–(c). The cation diffusion is similar. The migration energies for the cation and anion exchanges are very similar: 0.35–0.46 eV for the cation, 0.37–0.44 eV for the anion. This is less than the activation energy to move the BaO pair across the surface as a single adsorbed species ( $\approx 0.6$  eV) and comparable with the activation energy for similar movement of SrO ( $\approx 0.4$  eV). Despite the apparent similarity to the metal exchange reaction, there is a crucial difference – the necessity for the counterion to remain close to the exchanging ion. This suggests that extended subsurface diffusion mechanisms such as those proposed for metals<sup>2,4</sup> are unlikely for ionic surfaces.

Motion of ion pairs along a step at the (001) surface of BaO also proceeds by an exchange mechanism. However, the edge complicates matters because of the drastically reduced symmetry. The second stage of the exchange can move the ion pair towards, away from or parallel to the step. The energy barrier to moving the ion pair away from the step is slightly higher than the barrier to moving towards it, whilst the energy to move along the step is midway between these two. The energy to extract an ion from the step is relatively high ( $\approx 0.7$  eV), whilst the return energy is low ( $\approx 0.2$  eV). Ions in contact with the step edge are therefore bound to the step. They are able to move back and forth along the step by exchanging with ions in the step edge. However no exchange occurs with surface layer ions. As a result, clusters of ions or islands on the surface are very stable, and their evolution proceeds on a much longer timescale compared to the initial formation of proto-steps.

We calculated the activation energy for the different situations: movement of an BaO pair on the (100) BaO surface away from and near a step, and the same for an SrO pair on the (100) SrO surface. The activation energies for all of these processes have been used as input to kinetic Monte Carlo

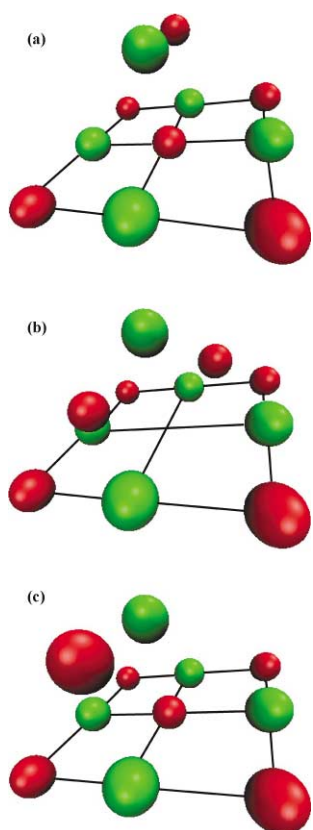


**Fig. 4** Exchange mechanism of the surface diffusion for the case of oxygen diffusion. Green spheres – cations, red spheres – oxygen ions. Shown are the initial position (a), middle of the transition (b) and the final position, after the exchange has taken place (c).

simulations. First the resulting isotropic two-dimensional diffusion coefficients can be extracted from these simulations from the standard result  $\langle r^2 \rangle = 4Dt$  where  $D$  is the diffusion coefficient. Diffusion coefficients are plotted as a function of inverse temperature in Fig. 5. The larger value of  $D$  is for the diffusion of SrO on SrO as would have been expected from the activation energies data. In order to demonstrate the importance of the exchange mechanism, we show in Fig. 5 the diffusion coefficient for the motion of BaO on BaO but *excluding* the exchanges. This results in a reduction of  $D$  by between one and three orders of magnitude, depending on temperature. A similar effect, although of smaller magnitude, was found for SrO on SrO.

Furthermore we can calculate the mean formation time of clusters and islands on the surface, starting from a random distribution of ion pairs. At the beginning of the KMC

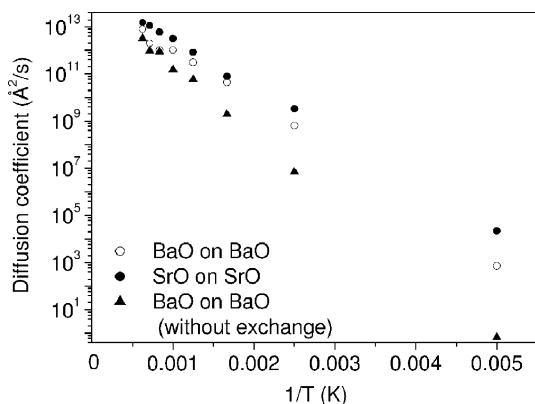


**Fig. 5** Diffusion coefficients for oxide ion pairs on the (100) surface of oxides as a function of inverse temperature: BaO on BaO (empty circles) and SrO on SrO (solid circles). The diffusion coefficient for BaO on BaO excluding the exchange mechanism is also shown for comparison (triangles).

simulation, randomly moving single pairs meet and create initial clusters, or proto-steps, which move much more slowly in our model; the proto-steps so produced attract molecules and other clusters in turn, resulting in the spontaneous creation of islands. We define the first stage of cluster formation as the stage when most of the single separate ion pairs form proto-steps (a proto-step here is any group consisting of more than one ion pair). Fig. 6 shows the average duration of the first stage for BaO. The starting point here was a random distribution of 100 Ba and O pairs on the  $20 \times 20$  BaO surface consistent with an overall coverage of 50%. Usually a few thousand elementary events are enough to reach a stable final configuration with one or more large clusters. Fig. 7 shows the average size of surface clusters of BaO (on BaO) and SrO (on SrO) as a function of coverage. For relatively small coverages, the final configuration consists of many small islands. With increasing coverage, the average size of an island increases and the total number of islands decreases. The evolution of the islands for BaO on BaO and a surface coverage of 30% is shown in Fig. 8.

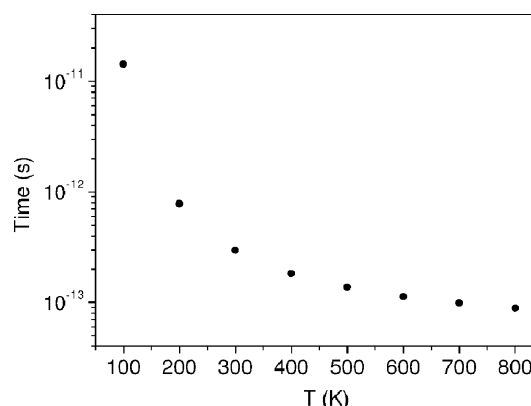


**Fig. 6** Average time taken by separate BaO pairs in an initial random configuration (surface coverage 50%) to form initial proto-steps as a function of temperature.

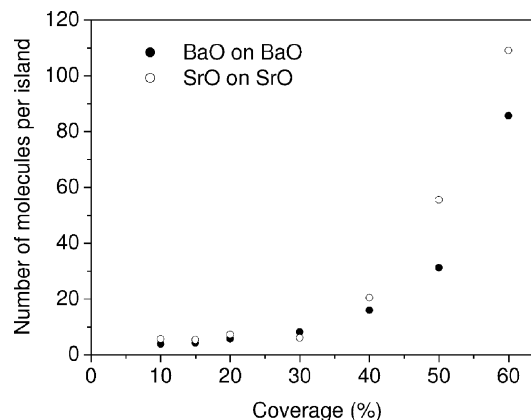


**Fig. 7** Average size of surface clusters of BaO and SrO after 20000 steps as a function of coverage.

## Conclusions

Interstitialcy mechanisms, the class into which our exchange mechanism essentially falls, are unusual in most bulk ionic materials. However, this is often because the Frenkel formation energies in the bulk are large, rather than because the interstitialcy migration energy itself is high. For an ionic pair at a surface, the initial condition for an interstitialcy mechanism is provided – there is no formation energy. The cooperative nature of the mechanism ensures that the Coulomb barrier to migration is low. The high energy cost of one ion climbing out of the Madelung well, which is a major factor in the high barriers to migration for ionic crystals, is largely offset by the

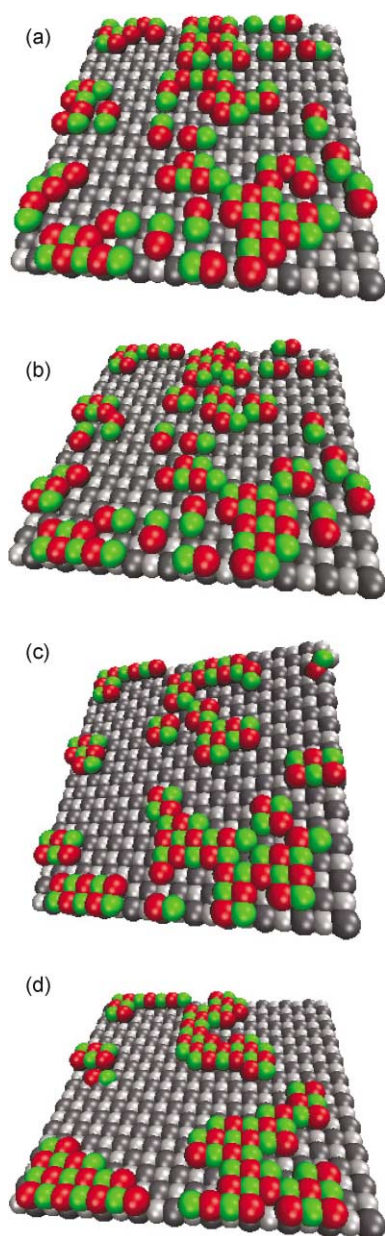


**Fig. 8** Formation of BaO islands on a BaO surface. Surface coverage is 30%. Shown are (a) the initial random configuration and snapshots after (b) 20, (c) 200 and (d) 20000 elementary steps.

energy gain of the other ion falling into the well as the first ion vacates it. Despite the similarity to the metal exchange reaction, there is an important difference – the necessity for the counterion to remain close to the exchanging ion.

We have shown the importance of exchange mechanisms in a variety of surface diffusion processes in simple oxides. The possibility of this kind of mechanism has been neglected in the past, despite the importance of well-defined layers of

crystalline oxides in solid state electronics.<sup>1</sup> More generally, molecular beam epitaxy is currently being used to create layered structures of ferroelectric, ferromagnetic and dielectric oxides.<sup>16</sup> The question of whether the exchange mechanism is still active when a molecule of one oxide diffuses on a different oxide substrate is of fundamental importance for creating sharp interfaces in such structures. The existence of this low-energy mechanism in some cases suggests that ionic materials may not be grown on a substrate with a similar structure without significant intermixing. Further investigations of this effect for the perovskite structures are in progress.

There are many possible applications of the techniques outlined in this paper, to more complex materials, surfaces and interfaces. The problem of reaching the timescales required will be particularly serious when simulating growth – generally molecular dynamics simulations of molecular beam epitaxy have to assume growth rates  $10^4$ – $10^6$  times those available to any experimentalist.

### Acknowledgements

The authors acknowledge funding from EPSRC under grant GR/R85969/01. Art Voter is thanked for access to his Temperature-Accelerated Dynamics code and for many useful conversations. The project used computational resources on the Mott machine at Rutherford–Appleton Laboratory and the Dirac machine at Bristol both funded by JREI grants.

### References

- 1 R. A. McKee, F. J. Walker and M. F. Chisholm, *Science*, 2001, **293**, 468.
- 2 R. Tromp, *Nat. Mater.*, 2003, **2**, 212.
- 3 G. L. Kellogg and P. J. Feibelman, *Phys. Rev. Lett.*, 1990, **64**, 3143; C. Chen and T. T. Tsong, *Phys. Rev. Lett.*, 1990, **64**, 3147.
- 4 J. Camarero, J. Ferrón, V. Cros, L. Gómez, A. L. Vázquez de Parga, J. M. Gallego, J. E. Prieto, J. J. de Miguel and R. Miranda, *Phys. Rev. Lett.*, 1998, **81**, 850.
- 5 D. C. Sayle, C. R. A. Catlow, J. H. Harding, M. J. F. Healy, S. A. Maicananu, S. C. Parker, B. Slater and G. W. J. Watson, *J. Mater. Chem.*, 2000, **10**, 1315.
- 6 See, for example, F. Shimojo and M. Aniya, *J. Phys. Soc. Jpn.*, 2003, **72**, 2702; Y. Yokoyama and M. Kobayashi, *Solid State Ionics*, 2003, **159**, 79.
- 7 G. Henkelman and H. Jónsson, *J. Chem. Phys.*, 2001, **115**, 9657.
- 8 G. Henkelman, B. P. Uberuaga and H. Jónsson, *J. Chem. Phys.*, 2000, **113**, 9901; H. Jónsson and G. Henkelman, *J. Chem. Phys.*, 2000, **113**, 9978.
- 9 M. R. Sørensen and A. F. Voter, *J. Chem. Phys.*, 2000, **112**, 9599.
- 10 F. Montalenti and A. F. Voter, *J. Chem. Phys.*, 2002, **116**, 481.
- 11 A. F. Voter, F. Montalenti and T. C. Germann, *Annu. Rev. Mater. Res.*, 2002, **32**, 321.
- 12 G. V. Lewis and C. R. A. Catlow, *J. Phys. C*, 1985, **18**, 1149.
- 13 P. P. Ewald, *Ann. Phys.*, 1921, **64**, 253.
- 14 For example: J. H. Harding, *Rep. Prog. Phys.*, 1990, **53**, 1403, and references therein.
- 15 M. J. Gillan, A. Manassidis and A. da Vita, *Philos. Mag. B*, 1994, 879.
- 16 D. G. Schlom, J. H. Haeni, J. Lettieri, C. D. Theis, W. Tian, J. C. Jiang and X. Q. Pan, *Mater. Sci. Eng. B*, 2001, **87**, 282.